Nuclei of the Primary Cosmic Radiation with $Z \geq 2$ at High Latitudes*

M. KOSHIBA† AND E. LOHRMANN‡
Department of Physics, University of Chicago, Chicago, Illinois

AND

H. AIZU§ AND E. TAMAI§
Department of Physics, Northwestern University, Evanston, Illinois

(Received 20 March 1963)

A large stack of nuclear emulsions was flown on 4 September 1959, near Sioux Falls, South Dakota, at an altitude of more than 135 000 ft. The stack was flipped at altitude. Stringent scanning criteria were applied. This allowed a determination of the Li Be B flux with very small uncertainties. 971 nuclei with $Z \geq 3$ were identified. The ratio L/M nuclei is 0.51 ± 0.07 at 200 MeV/$N < E <$ 700 MeV/N and 0.32 ± 0.03 at energies $>$700 MeV/N. This substantial increase of light nuclei with decreasing energy is found for all light nuclei Li, Be, and B. It is concluded that the amount of material traversed by the cosmic radiation before reaching the earth is larger for the slower particles. For the rest of the elements with $Z < 10$ the abundances do not change at low energies $<$700 MeV/N within statistics compared to results at high energies. Very little F is found at both high and low energies. C is found to be the most frequent element also below 700 MeV/N. Further results given are absolute flux values, the energy spectrum of light, medium, and heavy nuclei from 100 to 700 MeV/N and of α particles from 100 to 300 MeV/N. A cutoff energy of about 150 MeV/N is found for heavy primaries, much lower than the value calculated by Quenby and Wenk.

INTRODUCTION

STUDYING the composition and the energy spectrum of the heavy nuclei of the primary cosmic radiation has for many years been recognized as an important method of obtaining information about the origin of cosmic rays, and their propagation through space.

Problems which are well known and important in this connection are the abundance of Li, Be, and B, the ratio C:N:O, and the details of the charge spectrum of heavy elements.

In practice, experiments on the charge and energy spectrum of heavy primary nuclei face two major difficulties. The first difficulty concerns the extrapolation of the charge spectrum to the top of the atmosphere. The corrections to be applied are poorly known and are, unfortunately, quite big even if one has an exposure well above a pressure altitude of 10 g/cm^2. The second difficulty is the identification of the nuclei. This is particularly critical if one studies the flux of the nuclei at nonrelativistic energies, since one must measure at least two parameters of each track. It is mainly due to these difficulties that many conflicting results were obtained in the past. Only recently, a clearer picture began to emerge, as larger stacks of nuclear emulsion and high balloon flights became possible.

The first airm of the present experiment was to avoid both difficulties. The balloon flight was so high that corrections for Li, Be, and B were very small. In addition, the stack of nuclear emulsions was flipped by 90° when it had reached altitude to avoid corrections due to the ascent of the balloon. The size of the stack was such that the potential path length of all particles accepted in the scan were at least 12 cm. For most particles it was 20 cm. This greatly aided in identifying the particles. The second aim of the experiment was to obtain information about the flux of heavy nuclei at low energies, since most investigations up to now were done for relativistic energies of the particles, characteristically with exposures made in Texas. Therefore, our exposure was made at high geomagnetic latitudes, where the energy spectrum could be investigated down to energies of 200 MeV/nucleon. This low energy end of the spectrum is particularly interesting in connection with studies of the role of the sun and of the interstellar medium for the propagation of cosmic rays.[1]

EXPERIMENTAL PROCEDURE

1. Stack and Exposure

The stack of nuclear emulsions used for this experiment consisted of 300 pellicles, 15 cm×20 cm, 600-μ thick. In the center of the stack there were 280 sheets of type Ilford G5. At the bottom of the stack 10 sheets of Ilford K5 and 10 sheets of Ilford L4 were included. The stack was mounted in a gondola with 1.3-mm aluminum walls. It was surrounded by a 7.5-cm layer of styrofoam. The stack was mounted in a frame inside the gondola which could be flipped at the end of the ascent of the balloon. The timing mechanism consisted of a Haydon dc timing motor which, after a predetermined time, withdrew a lock and allowed the frame with the stack to rotate by 90°. It was then held in the

* Supported in part by a joint program of the U. S. Atomic Energy Commission and the Office of Naval Research and by the National Science Foundation.

† Present address: Institute for Nuclear Study, University of Tokyo, Tanashi, Tokyo, Japan.

‡ Present address: Deutsches Elektronen Synchrotron, Hamburg, Germany.

§ Present address: Rikkyo University, Tokyo, Japan.

[1] A preliminary account of this work was given by M. Koshiba at the Kyoto Conference [Proceedings of the Kyoto Conference, 1961 (unpublished)].

new position by a spring loaded lever fitting in a notch. In the new position which the stack maintained during the flight at the ceiling, the 20-cm edge of the stack was vertical.

The stack was launched on 4 September 1959 from Sioux Falls, South Dakota,[2] (geomagnetic latitude $\sim 53.5°$ N). The flight curve is shown in Fig. 1. The altitude was measured by a photobarograph and by a radiosonde. The stack was flipped 2.3 h after the launch, at an altitude of 115 000 ft (arrow in Fig. 1). At ceiling altitude the total amount of material above the top of the stack consisted of 1.5 g/cm^2 of residual atmosphere, 0.35 g/cm^2 aluminum, and 0.15 g/cm^2 styrofoam. The flight was terminated 8.8 h after the flipping of the stack near Harrison, Nebraska. The balloon had then covered about 360 miles on a westerly course.

2. Scanning

The 200 pellicles in the center of the stack were scanned along a line parallel to the top edge and 7 mm inside the stack. The scanning line had a length of 12 cm. It ended at a distance of 1.5 cm from either edge of the stack. Tracks having a projected zenith angle $\theta_p < 30°$ and a dip >4.4 mm/plate were accepted. However, in the first 4.5 cm and in the last 4.5 cm of the scanning line only tracks pointing away from the edges of the stack were accepted by choosing the projected zenith angle to be between 0° and 30° and 0° and −30°, respectively. This guaranteed a potential length for all tracks of >12 cm. In most cases it was ~ 20 cm. This was of great help in identifying the tracks.

All tracks accepted in the scan were required to have a grain density >80 grains/100μ. About 300 grains were counted on each track. To ensure the stability of this method, the scanners were required to make calibration counts on tracks of relativistic α particles at frequent intervals. The grain density of a relativistic α particle in this stack was 60 grains/100μ, for a relativistic Li track it was 110 grains/100μ, safely above our acceptance limit. Apart from all particles with

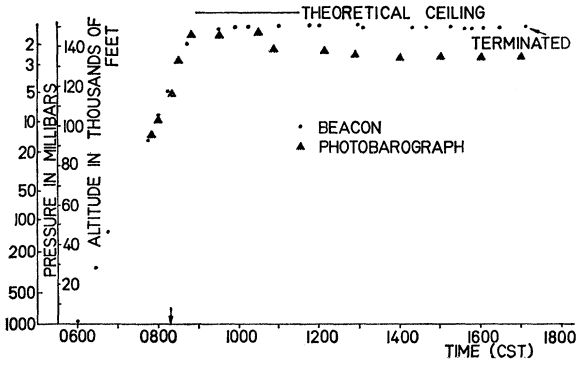

FIG. 1. Flight curve.

[2] We want to express our appreciation to the Raven Corporation for this excellent flight.

TABLE I. Corrections for extrapolating the flux to the top of the atmosphere.

Charge group	Scanning loss (%)	Loss by: Interaction in stack above scanning line (%)	Absorption and fragmentation in air (%)	Total correction factor
α	11.5	4.0	3.0	1.19
L	11.5	5.4	0.0	1.18
M	7	6.1	5.0	1.19
H	3	8.4	7.4	1.20

$Z \geqslant 3$, the scan accepted also α particles with an energy <400 MeV/N. The scanning efficiency and the consistency of the grain count was checked by a careful rescan of 19% of the total area. Values for the scanning efficiency are given in Table I.

An additional scan was made in 7 plates near the center of the stack to pick up all α particles and slow nuclei of charge one. The angle and dip criteria for this additional scan were the same. The grain density was required to be >40 grains/100μ. In this way α particles of all energies and singly charged particles with <200 MeV/nucleon were accepted.

Furthermore, the plates were scanned under low magnification very close to the upper end of the stack (~ 1 mm) for low-energy heavy nuclei, which stopped in front of the scanning line.

All tracks were traced until they interacted, stopped, or left the stack. In addition, all tracks were traced backwards to the top of the stack to eliminate those which originated in a fragmentation between the scanning line and the top of the stack.

The average thickness of one pellicle was 607μ, as obtained from a measurement of the total thickness of the assembled stack tightly clamped together. The beginning of the exposure is defined by the time the stack was flipped. The flux of particles crossing the scanning line prior to this moment is very small and can be neglected. For α particles the fraction is 1.8% and for heavier nuclei it is 1.2%. This is supported by the fact that only one definite and three possible cases of a heavy nucleus or an α particle apparently running backwards were found (among a total number of about 1200 particles). Therefore, the number of particles found in the main scan in the 200 plates corresponds to 79 m^2 sec sr.

3. Identification of the Tracks

The charge and energy of the heavy nuclei were determined by a combination of δ-ray counting, gap counting, and grain counting. The procedure was very similar to the one described elsewhere[3,4]; therefore,

[3] H. Aizu, Y. Fujimoto, S. Hasegawa, M. Koshiba, I. Mito, J. Nishimura, K. Yokoi, and Marcel Schein, Phys. Rev. **116**, 436 (1959).

[4] H. Aizu, Y. Fujimoto, S. Hasegawa, M. Koshiba, I. Mito, J. Nishimura, K. Yokoi, and Marcel Schein, Phys. Rev. **121**, 1206 (1961).

only a brief description will be given here. Since this paper is, in a sense, a continuation of earlier work, we have not included again the full details of the charge resolution and the results of the double identification of tracks.

A. *Stopping Tracks*

They were identified by counting δ rays both near the end of their range and at the point where they crossed the scanning line. For nuclei of charge $\leqslant 7$, δ rays which extended a projected distance $>2.2\mu$ from the track were counted. For charges $\geqslant 8$ this distance was increased to 4.7μ. At the end of the range an integral δ-ray count was performed over a distance of 3600μ for α particles and 2250μ for heavier nuclei. The integral number of δ rays found up to a certain distance from the stop is for nuclei of different charges related by a "similarity law" which was discussed in Ref. 3. Once a standard (for example, the group of α particles) is established, the relation can be predicted for the other nuclei. After correction for the background δ-ray density and development gradient, the predicted lines of integral δ rays versus range coincided with the experimentally found groups of tracks. For the extension of the method to nuclei of the H-charge group, the very distinct C group was used as a new standard.

The second independent information about the charge comes from the δ-ray count at the scanning line. Again, one makes use of a "similarity law" connecting the relation range versus δ rays for different charges (Ref. 3). The method was calibrated in three different ways:

(1) By measuring a large number of α particles and using the similarity law to predict the curves for heavier nuclei.

(2) By measuring this relation for several very long B, C, and N tracks and connecting the δ-ray count at the longest range to the calibration for relativistic tracks.

(3) By measuring a slow C breakup ($C \rightarrow 3\alpha$), without heavy prongs. The energy of this interaction could be established precisely from the range of the α particles.

All three methods agreed among themselves and with the calibration established from the integral δ-ray count. All heavy nuclei stops ($Z \geqslant 3$), whose range was long enough, were identified by both integral δ-ray count and the count at the scanning line. The double identification allows a separation of the charges up to $Z=9$. The α-particle stops were identified by the integral δ-ray count at the end of the range and (or) a restricted gap count (gap length $\geqslant 1.1\mu$) at the scanning line.

B. *Tracks Leaving the Stack*

They were identified by counting 4-grain δ rays about 1 cm inside the points where they entered and left the stack. The 20-cm length of the stack makes it possible to determine the energy of the nuclei up to 700 MeV/N. The calibration for this method was derived from the calibration for the relativistic tracks. For $Z \leqslant 4$ a restricted gap count (gaps $>1.1\mu$) was used instead of δ-ray counting. The gap count was calibrated by definite cases of relativistic α, Li, and Be tracks and the experimentally known relation range versus gap density for α particles.

C. *Tracks Interacting Inside the Stack*

The velocity of the heavy nuclei was measured by grain counting at least 2 singly-charged fragmentation products (protons, deuterons, tritons) of the original nucleus, and by mean gap length measurements of fragmentation α particles, when they were available. These fragmentation products were assumed to have about the same velocity as the original nucleus. The influence of fluctuations in the development for the grain count was eliminated by comparing it with the grain density of showers of high-energy particles in the same plate. In addition, the δ-ray density of the primary nucleus was determined at the interaction. For charges $Z \leqslant 8$, 4-grain δ rays were counted, and for $Z \geq 9$ δ rays extending a projected distance $>3.4\mu$ from the track. The calibration of the δ-ray count of the slow tracks was made by using the relation δ-ray density versus range obtained from the stopping tracks, and from a slow C breakup described in *a*. The δ-ray density for relativistic tracks was calibrated with the help of 7 charge-indicating interactions of B, C, N, and O tracks of high energy.

In order to extend the calibration established for the tracks with $Z \leqslant 8$ to the charge group with $Z \geq 10$, a number of tracks with charges from 6 to 12 were counted using both δ-ray criteria. In this way, a new calibration was established for the tracks with $Z=10-12$, using the $3.4\text{-}\mu$ δ-ray criterium. The measurement of the grain density or mean gap length of the singly-charged or doubly-charged fragmentation products yields the velocity of the nucleus, i.e., E/M. Together with the δ-ray density, one then obtains the charge of the nucleus from the relation δ-ray density versus E/M, which is known from the stopping tracks and from the relativistic tracks. The energy of the nucleus was then obtained from the measured δ-ray density only, by comparing it with the δ-ray density of relativistic tracks of the same charge. This method should be more reliable than using the grain count as an energy estimate. When no singly charged fragments were available or the results of the measurement was thought unreliable, the energy was estimated from the variation of δ rays with range.

D. *B and C Nuclei*

A special effort was made to separate B and C. All B tracks and those C tracks, whose identity was not considered to be definitely established, were remeasured

by independent observers. The main idea of this procedure was to reduce the number of C tracks wrongly identified as B tracks. Such a contamination is far more serious than the opposite effect, viz., B tracks among C, because of the large ratio C/B. There may still remain a small fraction of B nuclei wrongly identified as C, but due to the large number of C nuclei this can be neglected.

In addition, the δ-ray density was also measured at the scanning line. This served also to check for inconspicuous interactions which might have been overlooked during the tracing. For Li and Be tracks a restricted gap count was used for identification in addition to δ-ray counts.

The grain-, gap-, and δ-ray count was calibrated frequently by measuring standard events. In particular for the C–B separation, a standard track was counted before and after the measurement of each track.

4. Extrapolation to the Top of the Atmosphere

Due to the high altitude of this exposure and the small acceptance angle ($<30°$) the extrapolation of the charge and energy spectrum to the top of the atmosphere constitutes only a small correction. The correction for the energy loss in the atmosphere and in the gondola is straightforward. It corresponds to an equivalent range in emulsion of 0.8 cm.

Since in our scan tracks interacting above the scanning line were not included, the data must be corrected for interactions in the 0.7 cm of emulsions above the scanning line. For extrapolation from the top of the stack to the top of the atmosphere, the diffusion equations were used. Values for interaction lengths and fragmentation probabilities in emulsion and air were taken from Waddington's paper,[5] and the relative flux values of the α particles, L, M, and H (light, medium, and heavy) charge groups from the results of this work. The total path traversed in the atmosphere, the styrofoam insulation, and the gondola amounted to 2.1 g/cm^2, after correction for the average angle of incidence of the tracks.

In order to compare the abundances of the various groups of elements, a correction for scanning efficiency is also required, since it depends on the charge. The scanning efficiency was measured by rescanning as described earlier.

Table I lists all corrections which have been applied. Due to the small amount of material above the stack and the restriction to angles of incidence $<30°$, the correction for absorption and fragmentation in air is seen to be quite small. We have also calculated this correction with the NRL[6] set of fragmentation probabilities. The correction for L nuclei in this case is -2.5% instead of 0%. This indicates that in our experiment the uncertainty in the knowledge of the fragmentation probabilities is much smaller than the statistical errors and can be neglected.

[5] C. J. Waddington, Progr. Nucl. Phys. 8, 1 (1960).
[6] F. W. O'Dell, M. M. Shapiro, and B. Stiller, J. Phys. Soc. Japan **17**, Suppl. AIII, 23, (1962).

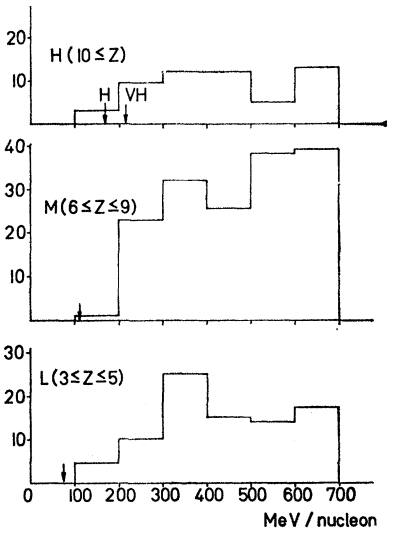

FIG. 2. Energy spectrum of L, M, and H nuclei at the top of the atmosphere. Arrows: air cutoff. Ordinate: number of particles in 100-MeV interval. To convert into flux (m^{-2}, sec^{-1} sr^{-1}), divide by 79, multiply by total correction factor of Table I.

RESULTS

Figure 2 shows the energy spectrum of the three charge groups $L(3\leq Z\leq 5)$, $M(6\leq Z\leq 9)$, and $H(Z\geq 10)$ between 100 and 700 MeV/N. The air cutoff is indicated by arrows. The correction for the energy loss in the material above the stack is included, so those are the spectra at the top of the atmosphere. The corrections for absorption, fragmentation, and scanning loss given in Table I are not included.

In Table II the details of the charge distribution are given. We have treated particles with energies $E>700$ MeV/N and 200 MeV/$N<E<700$ MeV/N separately, to detect differences in the energy spectra of various nuclei. The numbers given refer to the number of particles actually observed.

Table III shows the flux values extrapolated to the top of the atmosphere. The extrapolation was made with the correction factors from Table I. The various ratios between different charge groups are also shown.

TABLE II. Number of particles observed (uncorrected).

	Energy (MeV/N) $200<E<700$	$E>700$	All $E>200$
Li	28	39	67
Be	16	27	43
B	37	61	98
L group (LiBeB)	81	127	208
C	71	173	244
N	38	88	126
O	47	125	172
F	2	13	15
M group (CNOF)	158	399	557
H group $Z\geq 10$	51	155	206
VH group $Z\geq 19$	12	27	39

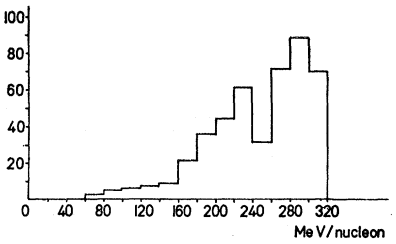

FIG. 3. Energy spectrum of α particles at the top of the atmosphere. Air cutoff is 50 MeV. Ordinate: number of particles in 20-MeV interval, corrected for absorption. To covert into flux (m^{-2} sec^{-1} sr^{-1}), divide by 71.

Figure 3 shows the energy spectrum of the α particles between 60 and 320 MeV/N at the top of the atmosphere. This spectrum was obtained from the range spectrum of stopping α particles, using an absorption mean free path for α particles of 19.9±1.2 cm.[7-9] When converting range into energy, we assumed that all particles with charge $Z=2$ were He^4.

DISCUSSION OF RESULTS

1. Light and Heavy Nuclei

During the last few years many investigations of primary heavy nuclei were carried out[3,4,6,9-21] (see also Refs. 9, 10, 15, and 19 for the earlier literature). It turned out that the altitude of the flight should be substantially above 10 g/cm² to become independent of the fragmentation correction for Li Be B nuclei. We shall, therefore, compare our results mainly with those obtained by O'Dell, Shapiro, and Stiller[6] with a very high flight over Texas, who also give a summary of results by other investigators, and with those of Refs. 3, 4, and 21 whose experiments were very similar to our own.

TABLE III. Flux values at the top of the atmosphere corrected according to Table I (m^{-2} sec^{-1} sr^{-1}).

Charge	Energy (MeV/N) 200<E<700	>700	>200
L (Li, Be, B)	1.22 ±0.13	1.91 ±0.17	3.13 ±0.22
M (CNOF)	2.38 ±0.19	6.00 ±0.30	8.38 ±0.35
H ($Z\geq 10$)	0.78 ±0.11	2.37 ±0.19	3.15 ±0.22
VH ($Z\geq 19$)	0.18 ±0.05	0.41 ±0.08	0.59 ±0.10
L/M	0.51 ±0.07	0.32 ±0.03	0.37 ±0.03
H/M	0.33 ±0.05	0.39 ±0.04	0.37 ±0.03
VH/M	0.076±0.02	0.068±0.02	0.070±0.02

TABLE IV. Comparison of ratios L/M and H/M (light nuclei/medium nuclei and heavy nuclei/medium nuclei).

Reference	L/M 200<E<700 (MeV/N)	L/M E>700 (MeV/N)	H/M 200<E<700 (MeV/N)	H/M E>700 (MeV/N)
This work	0.51±0.07	0.32±0.03	0.33±0.05	0.39±0.04
Ref. 6		0.25±0.05		0.38±0.04
Ref. 4	0.41±0.06		0.38±0.05	
Summary of Ref. 6		0.37		0.34
Ref. 22				0.38±004

Tables IV and V show a comparison of our results with those of Refs. 3, 4, and 6 and the summary of other papers given in Ref. 6. We have divided our results into a low-energy group (200 MeV/N<E/N <700 MeV/N) and a high-energy group (700 MeV/N <E/N). Our high-energy group corresponds roughly to the results of Ref. 6 obtained at the latitude of Texas.

The main result concerns the energy dependence of the abundance of the light elements. At energies <700 MeV/N we find an increase of the relative abundance of Li Be B nuclei by roughly a factor 1.7 compared to the abundance at high (>700 MeV/N) energies. This increase of the L nuclei with decreasing energy was already found in Refs. 3 and 4 and is now confirmed in a much higher flight and with increased statistics.

From Table V it can be seen that the increase takes place for all L nuclei Li, Be, and B by about the same amount. It is, therefore, very unlikely that this increase is caused by an energy dependence of the fragmentation probabilities as has already been discussed in Refs. 3

TABLE V. Comparison of the abundance of elements (relative to all nuclei with $Z\geq 3$ in %).

	NRL Ref. 6	Compilation of Ref. 6	This work 200<E<700 (MeV/N)	This work E>700 (MeV/N)	E>200 (MeV/N)
Li	5.3	5.2	9.7	5.7	6.9
Be	2.3	4.3	5.5	4.0	4.4
B	7.4	11.9	12.8	9.0	10.1
C	30.1	25.1	24.5	25.4	25.1
N	9.7	14.9	13.1	12.9	13.0
O	19.4	14.5	16.2	18.4	17.7
F	2.4	4.0	0.7	1.9	1.5
L	15.0	21.4	28.0	18.7	21.4
M	61.6	58.5	54.5	58.6	57.3
H	23.4	20.1	17.5	22.7	21.3

[7] G. Quareni and G. T. Zorn, Nuovo Cimento **1**, 1282 (1955).
[8] C. J. Waddington, Phil. Mag. **1**, 105 (1956).
[9] A. Engler, M. F. Kaplon, and J. Klarmann, Phys. Rev. **112**, 597 (1958).
[10] C. E. Fichtel, Nuovo Cimento **19**, 1100 (1961).
[11] R. R. Daniel and N. D. Prasad, J. Phys. Soc. Japan **17**, Suppl. AIII, 15 (1962).
[12] S. Biswas, P. J. Lavakare, K. A. Neelakantan, and P. G. Shukla, Nuovo Cimento **16**, 644 (1960).
[13] C. Q. Orsini, Nuovo Cimento **16**, 1040 (1960).
[14] C. M. Garelli, B. Quasiati, and M. Vigone, Nuovo Cimento **15**, 121 (1960).
[15] D. D. Kerlee, O. K. Krienke, Jr., J. J. Lord, and M. E. Nelson, Phys. Rev. **118**, 828 (1960).
[16] H. Hasegawa, Nuovo Cimento **23**, 292 (1962).
[17] F. B. McDonald and W. R. Webber, J. Phys. Soc. Japan **17**, Suppl. AII, 428 (1962).
[18] G. Kane, R. E. McDaniel, A. G. Barkow, and Z. O'Friel (unpublished).
[19] P. S. Freier, E. P. Ney, and C. J. Waddington, Phys. Rev. **113**, 921 (1959).
[20] R. R. Daniel and N. Durgaprasad, Suppl. Nuovo Cimento **23**, 82 (1962).
[21] D. E. Evans, Nuovo Cimento **27**, 394 (1963).

and 4. One concludes, therefore, that the amount of matter traversed by the low-energy particles before reaching the earth must be higher than for the high-energy particles and that the Fermi accelerating mechanism does not work in interstellar space at those low energies.

From this conclusion one would also expect that the ratio H nuclei/M nuclei decreases with decreasing energy. This is in accord with our own results (Table IV). The ratio H/M nuclei in the low-energy group is smaller than in the high-energy group by almost two standard deviations. Unfortunately, one finds in the literature a great variety of values for this ratio at high energies. However, our high-energy value of H/M is in very good agreement with the one found by O'Dell *et al.*[6] and with a careful revision of older published data by Waddington.[22] This strengthens our conclusion that the ratio H/M decreases somewhat with decreasing energy and goes together with the Li Be B result.

2. Element Abundances at High and Low Energies

In Table V we have further carried out a comparison of the abundance of the other elements with $Z<10$. The comparison is again made with the values of O'Dell *et al.* and their compilation of other values. In the high-energy group ($E>700$ MeV/N) our element abundances are in very good agreement with previous results and are generally between those of O'Dell *et al.* and the other authors. It should, however, be noted that we find a still smaller proportion of F. The abundances of the elements in the low-energy group are the same, within statistics, as those of the high-energy group, of course, with the exception of the L nuclei. In particular, we find also for the low-energy particles that carbon is more abundant than O and O more abundant than N. The number of F nuclei is also very small in the low-energy group and is consistent with zero. Similar results were found previously in Refs. 3 and 4.

3. Absolute Flux Values

Our flux values can be compared with those of Refs. 3 and 4 whose flight took place on 11 September 1957. We find that the flux of nuclei of the low-energy group <700 MeV/N found by us is substantially smaller than the one found on 11 September 1957. For example, we found that our value of the flux of M nuclei is smaller than theirs by about a factor of 1.6. The flux values at higher energies >700 MeV/N are in fair agreement.

The same effect exists for the α particles, for which we can compare the flux values in the energy interval from 100 MeV/N to 300 MeV/N. Our flux is smaller than the one found by Ref. 4 by a factor of 2.4. This larger factor is understandable, since for the α particles we compare only the lowest energy intervals. Our ratio M nuclei/α particles in the range from 100 MeV/N to 300 MeV/N is $(7.2\pm1.4)\%$, to be compared with $(8.7\pm1.4)\%$ (between 200 MeV/N and 700 MeV/N) from Ref. 4. From these data we conclude that the flux of heavy nuclei below 700 MeV/N on 4 September 1959 was down by about a factor 1.6 compared to the flux on 11 September 1957, whereas no substantial change could be seen for the higher energies. The change affected all nuclei in about the same way.

4. Cutoff Energies

The lowest energies which were observed for nuclei with $Z\geqslant3$ were 140 MeV/N, extrapolated to the top of the atmosphere. This is well above our air cutoff for L and M nuclei. The spectrum of the α particles goes down even to 70 MeV/N. The discrepancy with the heavy nuclei cannot be explained by assuming a certain percentage of the He^3 among the helium nuclei.[23,24] However, due to insufficient statistics for the nuclei with $Z\geqslant3$, the discrepancy might not be real.

Our experimental cutoff energies can be compared with the new calculation of Quenby and Wenk.[25] With the help of a table of vertical cutoff energies given by these authors, the theoretical cutoff energies were found to be 330 ± 30 MeV/N at Sioux Falls, South Dakota and $540+50$ MeV/N at Harrison, Nebraska for nuclei with $Z/A=1/2$. According to Fig. 2, we find an appreciable flux of heavy nuclei below the lowest cutoff energy of 300 MeV/N allowed by the calculations of Quenby and Wenk. Only more observations at different times will probably be able to clarify the reasons for the discrepancy. Apart from our results, there also seem to be other observations of particles below the geomagnetic threshold, e.g., Ref. 26.

Also observed in the stack was a substantial flux of singly-charged primary particles below the expected geomagnetic cutoff energy, whose spectrum shape is rather similar to that of protons in the inner Van Allen belt. It seems suggestive to consider the geomagnetic cutoff at these latitudes as being switched on and off depending on the disturbances, probably of solar origin. The parts on the He^3, He^4, and the singly charged component will be published in a separate paper.

5. Negative Results

We have investigated 971 tracks of nuclei with $Z\geqslant3$ in this work. We found no nucleus with charge >28. Taken together with other systematic investigations,

[22] C. J. Waddington, Phil. Mag. **5**, 311 (1960).

[23] M. V. K. Appa Rao, Phys. Rev. **123**, 295 (1961).

[24] M. V. K. Appa Rao, J. Geophys. Res. **67**, 1289 (1962).

[25] J. J. Quenby and G. J. Wenk, Phil. Mag. **7**, 1457 (1962).

[26] F. B. McDonald, Phys. Rev. **116**, 462 (1959).

this leads to a very low limit of abundance of elements heavier than the iron group. This is also in agreement with satellite results of Kurnosova *et al.*[27]

Two hundred and ninety of the heavy nuclei had energies <700 MeV/N. In addition, we found 227 stopping α particles. Any antiparticle among this group would have certainly been identified. None was found.

[27] L. V. Kurnosova, L. A. Rozorenov, and M. I. Fradkin. Iskusst. Sputniki Zemli **2**, 70 (1958).

ACKNOWLEDGMENTS

The authors are deeply indebted to the late Professor M. Schein, who initiated this investigation and made it possible for us to carry it through. They are also thankful to Professor J. H. Roberts from Northwestern University for the interest and support given to us. D. M. Haskin provided valuable technical help and contributed greatly to the design and construction of the flipping mechanism. We also thank the scanners of our laboratories for their patient work.

PHYSICAL REVIEW VOLUME 131, NUMBER 6 15 SEPTEMBER 1963

Empirical Relations Involving the Hyperons and Baryon Isobars*

R. M. STERNHEIMER
Brookhaven National Laboratory, Upton, New York
(Received 12 April 1963; revised manuscript received 22 May 1963)

A scheme for the classification of the nucleon isobars recently proposed by Kycia and Riley is extended to include the hyperon isobars Y_0^* and Y_1^* with strangeness $S=-1$. The present model is essentially based on the existence of empirical mass relations involving the various baryon isobar states. The extent of the validity of these mass relations is discussed. A classification of the six isobar systems which occur in the present scheme is described. We also discuss the set of quantum numbers which is necessary to characterize an isobaric state.

I. INTRODUCTION

IN a recent paper, Kycia and Riley[1] have discussed several interesting mass relations which enabled them to classify the nucleon and the known nucleon isobars into two systems, with the nucleon and the $I=J=\frac{3}{2}$ isobar as the ground states of the two systems. Subsequently, Sternheimer[2] pointed out some additional mass relations involving the hyperons and baryon isobars.

In Sec. II of the present paper, we will discuss a scheme similar to that of Kycia and Riley, which enables one to classify the Y_0^* and Y_1^* isobars of strangeness $S=-1$. The present model is essentially based on the existence of an empirical mass sum relation, according to which the mass of an isobar is equal, to a good accuracy, to the sum of the masses of a baryon ground state and one or several mesonic particles. In Sec. III, the extent of the validity of the mass relation is investigated.

In Sec. IV, it will be shown that the mass relation is also valid for several mesonic particles (including the η meson), which can be regarded as combinations of a small number of pions. In Sec. V, we will discuss a possible interpretation of these empirical results, as indicating that the baryon isobars can be considered as loosely bound nuclei consisting of an unexcited baryon plus one or several mesonic particles. A similar interpretation can be given for the π meson combinations which are used as constituents of some of the isobars in the present scheme.

In Sec. VI, a classification of the isobar systems is proposed. It is also pointed out that the number of two-particle thresholds which do not lead to a maximum in the total πN or $\bar{K}N$ cross section greatly exceeds the number of thresholds which can be correlated with such a maximum (isobar formation). This fact may indicate the existence of a selection rule which determines under what conditions a given baryon state and mesonic particle can combine to form an isobar. In Sec. VII, we examine the set of quantum numbers which is necessary in order to characterize an isobaric state. It is found that the set I, J, L, S (I=isotopic spin, J =total angular momentum, L=orbital angular momentum, S=strangeness) will, in general, be necessary and sufficient to define an isobaric state, i.e., there will be, at most, one isobar with given values of I, J, L, and S. This result indicates that there is probably no analog to a radial (principal) quantum number for the baryon isobars.

Finally, in Sec. VIII, we discuss, in general terms, some of the properties of the present model. In connection with the present paper and Ref. 1 and 2, it should be noted that for a few baryon resonances, the fact that they correspond to thresholds for two-particle produc-

* Work performed under the auspices of the U. S. Atomic Energy Commission.
[1] T. F. Kycia and K. F. Riley, Phys. Rev. Letters **10**, 266 (1963).
[2] R. M. Sternheimer, Phys. Rev. Letters **10**, 309 (1963).